

Multi-Temperature Analysis of a Sigmoidal Active Region

HORI Kuniko, HARRA Louise K.¹, MOORE Ron L.² and FALCONER David A.²

Solar Observatory, National Astronomical Observatory of Japan, Tokyo 181-8588, Japan

¹ *Mullard Space Science Laboratory, University College London, Dorking, Surrey, RH5 6NT, UK*

² *NASA Marshall Space Flight Center, Huntsville, AL 35812, USA*

(Received: 14 November 2004 / Accepted: 26 August 2005)

Abstract

A sigmoidal structure on the solar surface, which is generally remarkable in soft X-ray images, is known as a manifestation of highly sheared magnetic loops. It often marks the source region of a coronal mass ejection (CME) that can disturb Earth's geomagnetosphere and then atmosphere. Previous observational studies on the solar sigmoids have focused on their topology (*e.g.*, accumulation of magnetic helicity or shear) and connection with CMEs (*e.g.*, missing mass deduced from a dimmed area in 2D solar images) on the basis of soft X-ray images, *i.e.*, emission from coronal hot plasmas (> 2 MK). We investigate a sigmoidal active region using the Coronal Diagnostic Spectrometer (CDS) instrument on the Solar and Heliospheric Observatory (*SOHO*) spacecraft stationed at the L1 Lagrangian point. CDS can provide both images and spectra of extreme ultraviolet (EUV) emission lines that cover formation temperatures in the range $10^4 - 10^6$ K. By combining CDS images with images in other wavelengths, we diagnose multi-temperature structure of a sigmoidal active region.

Keywords:

Sun, corona, transient region, magnetic field, EUV line, sigmoid

1. Introduction

Solar eruptive phenomena such as flares, filament eruptions, and coronal mass ejections (CMEs) are deeply involved with sheared (or twisted) magnetic structures that store extra magnetic energy in them. Especially, sigmoidal active regions that appear in a shape of a character "S" or "inverted-S" are known to be a possible CME source [1, 2]. Hence, sigmoids belong to an important category for the *space weather* forecast. The soft X-ray telescope (SXT) on the Japanese *Yohkoh* spacecraft observed many sigmoids that partially or bodily erupted and left a cusp or an arcade-like structure. The sigmoid disappearance is often followed by an appearance of localized dark areas (so-called *dimming*) around the eruption site (*e.g.*, [3]). While the cusp and arcade structures suggest the occurrence of magnetic reconnection, the dimming suggests a decrease of coronal mass due to the eruption or a temperature change in the area (*e.g.*, [4]). Information provided by the *Yohkoh* SXT is, however, limited to hot plasmas (> 2 MK) in the corona. The physical process involved in a sigmoid formation is thus still not well addressed. (For possible scenarios, see, *e.g.*, [5 - 7]).

Here we discuss a magnetic configuration of a sigmoidal active region using extreme ultraviolet (EUV)

spectroscopic observations with the Normal Incidence Spectrometer (NIS) of the Coronal Diagnostic Spectrometer (CDS) on the Solar and Heliospheric Observatory (*SOHO*) spacecraft [8]. The CDS can address plasma characteristics (density, temperature, and velocity) within a single volume from the chromosphere through to the corona. By comparing sigmoids in CDS and SXT images, Gibson *et al.* [9] reported that CDS sigmoids have the same helical orientations as their X-ray counterparts. Multi-wavelength observations can prove 3D structure of sigmoids as they are sensitive to temperatures. In addition to CDS and SXT images, we also use magnetograms from *SOHO*/MDI (Michelson Doppler Imager) and NASA/MSFC (Marshall Space Flight Center). Cool structures (filaments) are verified with H_{α} images from Hiraiso Solar observatory.

2. Observations

The target sigmoidal active region was NOAA #9254, which we selected for an international campaign observation involving the instruments on the *SOHO* spacecraft, coordinated among ground-based observatories in Japan. The observation period was December 6–9, 2000. Figure 1 left shows a soft X-ray snapshot of

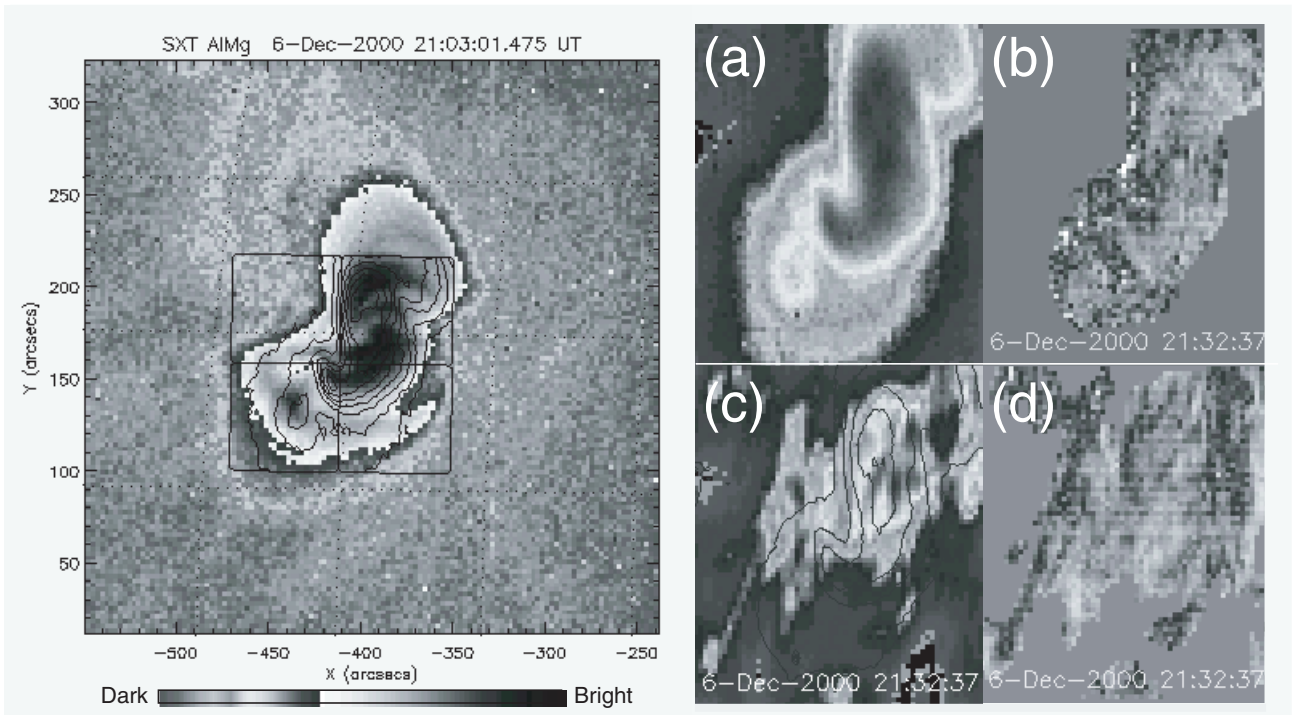


Fig. 1 Snapshots of AR9254 from SXT (left) and CDS (right) at 21h (UT) on Dec. 6, 2000. The CDS images show intensity (a, c) and velocity (b, d; up to $\pm 30 \text{ km s}^{-1}$) distributions in Fe XVI line (a, b) and in O V line (c, d). The contours on the SXT image and in panel (c) outline the sigmoid in panel (a). The color bar attached in the bottom left shows the intensity scales. Solar north is up and west to the right.

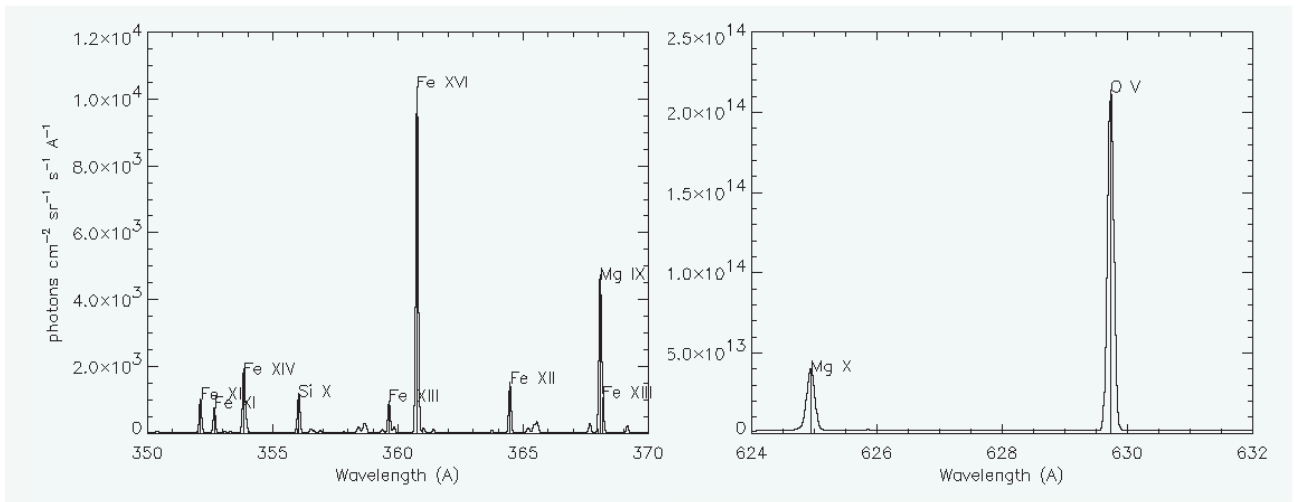


Fig. 2 Synthetic spectrum for a typical active region with a constant density of 10^{10} cm^{-3} . Created by CHIANTI database [10], [11].

AR9254 taken at 21:03 UT on Dec 6 from the SXT. The region consists of several low-lying bright loops (shown in black, see the color bar attached in the bottom) and faint tall loops lying outside or above the bright loops. The low-lying loops as a whole form an S shape. Each loop has footpoints in positive (right-hand or west side) and negative (left-hand or east) magnetic polarity fields. Thus the S-arrangement almost traces the magnetic neutral line that separates the opposite magnetic polarities. The boxed area shows the CDS field-of-view,

$122'' \times 121''$ ($\sim 89000 \text{ km}$), which was rastered with the CDS long slit. The CDS observed AR9254 from 0h to 4h (UT) on each day with a time resolution of 30 minutes in 10 spectral lines that are listed in Table 1. These lines were selected to cover a wide range of temperatures from the transient region ($> 10^4 \text{ K}$) to the corona ($> 1 \text{ MK}$). Figure 2 shows spectrum for two spectral ranges that were calculated by CHIANTI database for a typical active region with a constant density of 10^{10} cm^{-3} [10, 11].

Table 1 Observed Spectral Lines.
(* Corresponding to a 2nd-order emission line.)

Ion	WL(Å)	Transition	T (MK)
Fe XVI	361	$3s^2 S_{1/2} - 3p^2 P_{1/2}$	2.5
Si XII	521	$1s^2 2s^2 S_{1/2} - 1s^2 2p^2 P_{1/2}$	2.0
Mg X	610	$1s^2 2s^2 S_{1/2} - 1s^2 2p^2 P_{3/2}$	1.3
Mg IX	368	$2s^2 ^1S_0 - 2s 2p ^1P_1$	1.0
Ca X	558	$3s^2 S_{1/2} - 3p^2 P_{3/2}$	0.6
Ne VI	563	$2s^2 2p^2 P_{3/2} - 2s 2p^2 D_{5/2}$	0.4
O V	630	$2s^2 ^1S_0 - 2s 2p ^1P_1$	0.3
O III	600	$2s^2 2p^2 ^1D_2 - 2s 2p^3 ^1D_2$	0.1
He II*	608		
He I	584	$1s^2 ^1S_0 - 1s 2p ^1P_1$	0.03

In SXT full-disk images, AR9254 became active on Dec 6, but no major flare activity was reported. The enhanced activity was also observed in other wavelengths. The MSFC vector magnetograph showed a development of a magnetic shear along the magnetic neutral line, which almost coincides with the central part of the sigmoid. In this region, $H\alpha$ brightenings were intermittently observed during the four observation days. On Dec 7, an $H\alpha$ filament rooted in a positive preceding spot apparently extended its length northward along the magnetic neutral line. The filament formed a kinked structure on Dec. 8, while in SXT images a tall cusp appeared to stride across the sigmoid.

The CDS high temperature line (Fe XVI; 2.5 MK) images show both formation and decay processes of the sigmoid. In lower temperature lines, on the other hand, the active region appeared as a double ribbon along the sigmoid (Si XII, Mg X; 1–2 MK) or patches around the center of the sigmoid (Ne VI and O V; 0.2–0.4 MK). Figure 1 right panels show CDS images in Fe XVI line (a and b) and in O V line (c and d) taken at 21:32 UT on Dec 6 when the sigmoid was most clearly seen. The panels (a) and (c) show intensity distributions (see the color bar), and the panels (b) and (d) show velocity distributions. In the velocity maps, black and white colors correspond to blue- and red-shifts up to $\pm 30 \text{ km s}^{-1}$, respectively (low emission region was masked). Clear line-of-sight flows were detected only in Fe XVI and O V emission lines. The Fe XVI map (b) shows upward and downward flows along the left- and right-edge of the sigmoid, respectively. In the O V map (d), there are upward motions outside of the sigmoid. After Dec 7, the brightness of AR9254 gradually faded in all wavelengths.

3. Discussion

By comparing the CDS and SXT images, it is clear that our sigmoid was not an S-shaped *single* loop that was bodily formed and emerged from beneath the photosphere as demonstrated by numerical simulations (*e.g.*, [6]). Instead, it consisted of sheared loops lying below the tall loops that have more or less potential-field like shapes. The SXT observed a cusp structure on Dec. 8, which presumably emerged from one of the tall loops. Figure 3 illustrates a possible magnetic configuration of AR9254. The oblique-lined and gray areas correspond to negative and positive magnetic polarities, respectively. The three characteristic features observed with CDS correspond to vertical slices of the sigmoidal active region that consists of a pair of piled arcade loops: The inner (low-lying) arcade loops (indicated by the dashed parallelogram) apparently form the hot ($> 2 \text{ MK}$) sigmoid. In the upper transition region, the footpoints of both inner and outer (tall) arcade loops might appear as the double ribbon due to heat conduction (*e.g.*, [12]). In the lower transition region, the heat conduction is less effective and thus footpoints of only active loops might appear as the bright patches.

Del Zanna *et al.* [13] diagnosed an evolution of a sigmoidal active region with CDS. They found postflare upflows ($\sim 30 \text{ km s}^{-1}$) in coronal lines (Mg X, Si XII) at the two ends of the sigmoid. They argued that these upflows might be *chromospheric evaporation* following the flare energy release. Because of the limited data set,

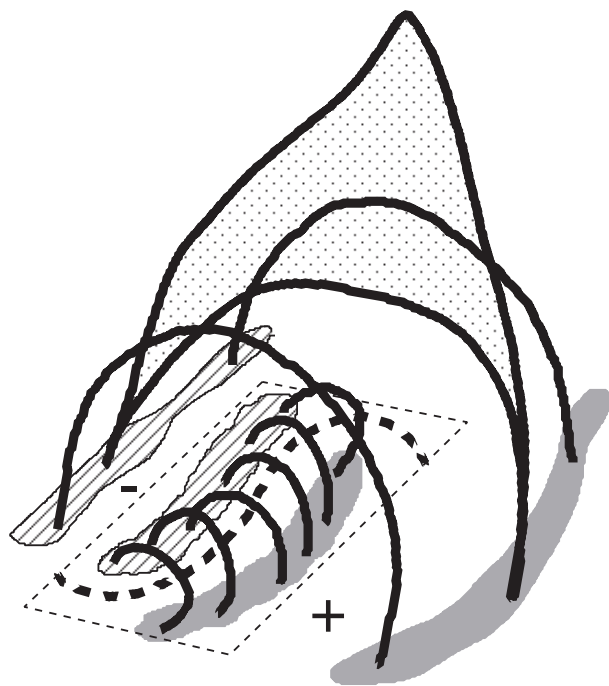


Fig. 3 Schematic magnetic configuration of AR9254.
(For details, see text.)

we could not specify the start and end times of the minor flare activity in AR9254 on Dec. 6–9. However, we conjecture that the flows detected in AR9254 were associated with some energy release during the activity. As the next step, we will calculate the accumulation of currents along the magnetic neutral line from the MSFC vector magnetograph [14], which is expected to be largest just before the flare on Dec. 6. Considering the direction of plasma flows, we will also try to specify the energy release site within AR9254.

References

- [1] D.M. Rust and A. Kumar, *ApJL* **464**, L199 (1996).
- [2] R.C. Canfield, H.S. Hudson and A.A. Pevtsov, *IEEE* **28**, No. 6, 1786 (2000).
- [3] A. Sterling and H. Hudson, *ApJL* **491**, L55 (1997).
- [4] L.K. Harra and A. Sterling, *ApJ* **587**, 429 (2003).
- [5] R.L. Moore, A.C. Sterling, H.S. Hugh, J.R. Lemen *ApJ* **552**, 833 (2001).
- [6] R. Matsumoto, T. Tajima, W. Chou, A. Okubo and K. Shibata, *ApJL* **493**, L43 (1998).
- [7] P.C.H. Martens and C. Zwaan, *ApJ* **558**, 872 (2001).
- [8] R.A. Harrison, *et al.* *Sol. Phys.* **162**, 233 (1995).
- [9] S.E. Gibson, H.E. Mason, D. Pike and P.R. Young, *Plasma Dynamics and Diagnostics in the Solar Transition Region and Corona*, eds. J.C. Vial and B. Kaldeich-Schurmann, ESA publications, Noordwijk, 331 (1999).
- [10] K.P. Dere, E. Landi, H.E. Mason, B.C. Monsignori Fossi and P.R. Young, *AASS* **125**, 149 (1997).
- [11] P.R. Young, G. Del Zanna, E. Landi, K.P. Dere, H.E. Mason and M. Landi, *ApJS* **144**, 135 (2003).
- [12] A. Czaykowska, B. De Pontieu, D. Alexander and G. Rank, *ApJL* **521**, L75 (1999).
- [13] G. Del Zanna, H.E. Mason, S.E. Gibson, C.D. Pike and C.H. Mandrini, *Adv. Space Res.* **30**, No. 3, 551 (2002).
- [14] D.A. Falconer, *JGR* 106 (All), 25185 (2001).